Habitable Planet, 2025, 1(1&2):171–184

Habitable Planet

Journal Homepage: www.habitableplanetjournal.com

Climatic shifts and floristic responses during India's tectonic voyage from Gondwana to Asia

Gaurav Srivastava* and Harshita Bhatia

Birbal Sahni Institute of Palaeosciences, 53 University Road, Lucknow 226 007, India

ABSTRACT

Rising atmospheric carbon dioxide (CO_2) levels are profoundly altering Earth's hydrological systems. To contextualize these changes, insights from past warm intervals are essential. This study synthesizes plant-derived proxy records from the Indian subcontinent to reconstruct hydrological patterns from the Late Cretaceous through the Paleogene—a period marked by India's tectonic drift from Gondwanaland to Asia. We synthesize climatic trends based on results obtained through quantitative methodology including Climate Leaf Analysis Multivariate Program (CLAMP), Coexistence Approach (CA), and stable isotope analyses. Results indicate a persistently warm and humid climate with high mean annual precipitation and pronounced seasonal rainfall from the latest Cretaceous into the early Paleocene. Throughout the early to middle Paleogene, including hyperthermal events such as the PETM, ETM-2, and MECO, plant assemblages reflect changes in hydrological cycles and biotic turnover. Notably, these intervals saw a rise in deciduous taxa, signaling heightened seasonality and prolonged dry periods despite global warming. The Early Eocene Climatic Optimum (EECO) stands out for its sustained warm and humid conditions that supported stable tropical evergreen rainforests. The long-standing monsoonal regime observed during Late Cretaceous to early Oligocene more closely resembled the present-day Indonesian–Australian Monsoon than the modern South Asian Monsoon, which likely developed following Himalayan uplift in the Neogene. This synthesis highlights the complex interplay between global warming, seasonal precipitation patterns, and vegetation dynamics, reinforcing India's key role in understanding Cenozoic climate–biosphere evolution.

ARTICLE INFO

History:
Received Jun 02, 2025
Revised Jun 27, 2025
Accepted Jun 28, 2025

Keywords:
Hyperthermal
Monsoon
Paleogene
Hydrological cycles

Citation:
Srivastava, G., Bhatia, H., 2025. Climatic shifts and floristic responses during India's tectonic voyage from Gondwana to Asia. Habitable Planet 1(1&2), 171–184.
https://doi.org/10.63335/j.hp.2025.0014.

Research highlights

- Characterized Late Cretaceous–Paleogene hydrology from Indian plant fossil data.
- PETM, ETM-2 and MECO shows increased deciduous taxa and rainfall seasonality.
- EECO supported stable tropical evergreen rainforests under humid conditions.
- Indian monsoon resembled I-AM type until SAM emerged after Himalayan uplift.

*Corresponding author. Email: gaurav_jan10@yahoo.co.in (GS), bhatiaharshita2013@gmail.com (HB)

1 Introduction

Global climate is changing due to an unprecedented increase in atmospheric carbon dioxide (CO_2) concentrations (Osman et al., 2021). While warming typically intensifies the hydrological cycle, it does not necessarily make the world wetter (Pierrehumbert, 2002). Recent advances in climate modelling have enabled researchers to disentangle the complex relationship between warming and the hydrological cycle (Held and Soden, 2006). To reduce uncertainties and enhance the precision of future climate projections, long-term proxy data from the past are essential. In this context, climate and biotic records from the Late Cretaceous–Paleogene are particularly valuable for understanding the interactions between warming, the hydrological cycle, and their impacts on biota (Zachos et al., 2008; Bhatia et al., 2021; Srivastava et al., 2023, 2024).

The Indian plate, present-day India, undertook a remarkable tectonic journey from Gondwanaland to Asia, spanning approximately 9,000 km for 160 million years. This movement occurred at varying speeds—around 20 cm/year from the Late Cretaceous to early Eocene, slowing to about 5 cm/year following its collision with the Eurasian plate (Chatterjee et al., 2013; Pusok and Stegman, 2020) (Fig. 1A–D). During this voyage, India acted both as a "biotic ferry" and as a homeland for diverse biota (Bossuyt and Milinkovitch, 2001; Rose et al., 2014; Wheeler et al., 2017; Kapur and Khosla, 2018). Owing to its passage through a broad range of latitudes, India experienced a variety of climatic regimes, making it a natural laboratory for geoscientists to investigate the evolving patterns of climate and biota through geological time, especially in low-latitude settings. Notably, India encountered several key geological and climatic changes during its journey, including the Cretaceous–Paleogene (K–Pg) boundary, the Paleocene–Eocene Thermal Maximum (PETM), Eocene Thermal Maximum 2 (ETM-2), the Early Eocene Climatic Optimum (EECO), the Middle Eocene Climatic Optimum (MECO), and the late Eocene–early Oligocene transition. Various studies have attempted to quantify India's paleoclimate during these intervals to better understand the relationship between climatic oscillations and vegetation shifts (Srivastava et al., 2012, 2023, 2024; Samanta et al., 2013; Shukla et al., 2014; Bhatia et al., 2021; Deori et al., 2025).

This paper examines changes in the hydrological cycle across the Late Cretaceous to Paleogene in the Indian subcontinent, a period of significant climatic and tectonic transitions influenced by the northward drift of the Indian Plate and the Deccan volcanism (Chatterjee et al., 2013; Bhatia et al., 2021). Despite extensive plant fossil records from this interval (Srivastava et al., 2012, 2023, 2024; Samanta et al., 2013; Shukla et al., 2014; Bhatia et al., 2021; Deori et al., 2025), a systematic synthesis of biotic proxy evidence related to hydrological change remains absent. Plant-based proxies, such as leaf morphology, palynological assemblages, and fossil wood anatomy, offer valuable but indirect insights into regional precipitation patterns and moisture availability. However, these proxies often reflect complex ecological responses and are influenced by varying temporal and spatial resolutions. Here, we compile diverse plant-derived proxy data from multiple basins across India, focusing on shifts in vegetation structure, diversity, and physiological traits. This synthesis enables a quantitative assessment of hydrological variability and helps contextualize regional climatic responses to global events such as the K–Pg boundary and early Paleogene warming within the evolving paleogeographic framework of the Indian subcontinent.

2 The Late Cretaceous to early Paleocene climate of India

The climate of the Late Cretaceous to early Paleocene in peninsular India has been primarily inferred from the Deccan Intertrappean sediments, which are preserved within the Deccan Volcanic Province (DVP). The DVP is one of the largest igneous provinces on Earth, covering approximately 500,000 km² of peninsular India, and potentially extending up to 1.5 million km² when including associated marine deposits in the Arabian Sea (Jay and Widdowson, 2008; Kale, 2020). This extensive volcanic activity is attributed to the northward movement of the Indian plate over the Réunion hotspot. Composed predominantly of tholeiitic basalts, the DVP is notable not only for its immense volume of lava output (∼2.5 million km³) but also for its timing, which is closely associated with the Cretaceous–Paleogene (K–Pg) boundary. High-precision $^{40}Ar/^{39}Ar$ dating indicates that volcanic eruptions occurred quasi-continuously for approximately 991,000 years, from ∼66.4 Ma to ∼65.4 Ma (Sprain et al., 2019). Geographically, the DVP is subdivided into three major sub-provinces: the Malwa, Mandla, and Central Deccan lobes. Palaeogeographic reconstructions suggest that during the deposition of these sediments, the Indian subcontinent was located at a palaeolatitude of approximately 16° S (https://www.odsn.de/).

Several paleoclimatic reconstructions have been attempted using plant-based proxies from the Deccan Intertrappean beds, particularly within the Mandla lobe (Fig. 2). Bhatia et al. (2021) employed the Climate Leaf Analysis Multivariate Program (CLAMP) (Tables 1 and 2) to assess the climate of this region during the latest Maastrichtian to earliest Danian. Their analysis indicates a high mean annual precipitation (MAP) of 232 ± 64 cm, with pronounced rainfall seasonality between the summer and winter months. The cold month mean temperature (CMMT) was estimated at 17.2 ± 3.5 ℃, suggesting a warm, tropical to subtropical climate regime. Complementary reconstruc-

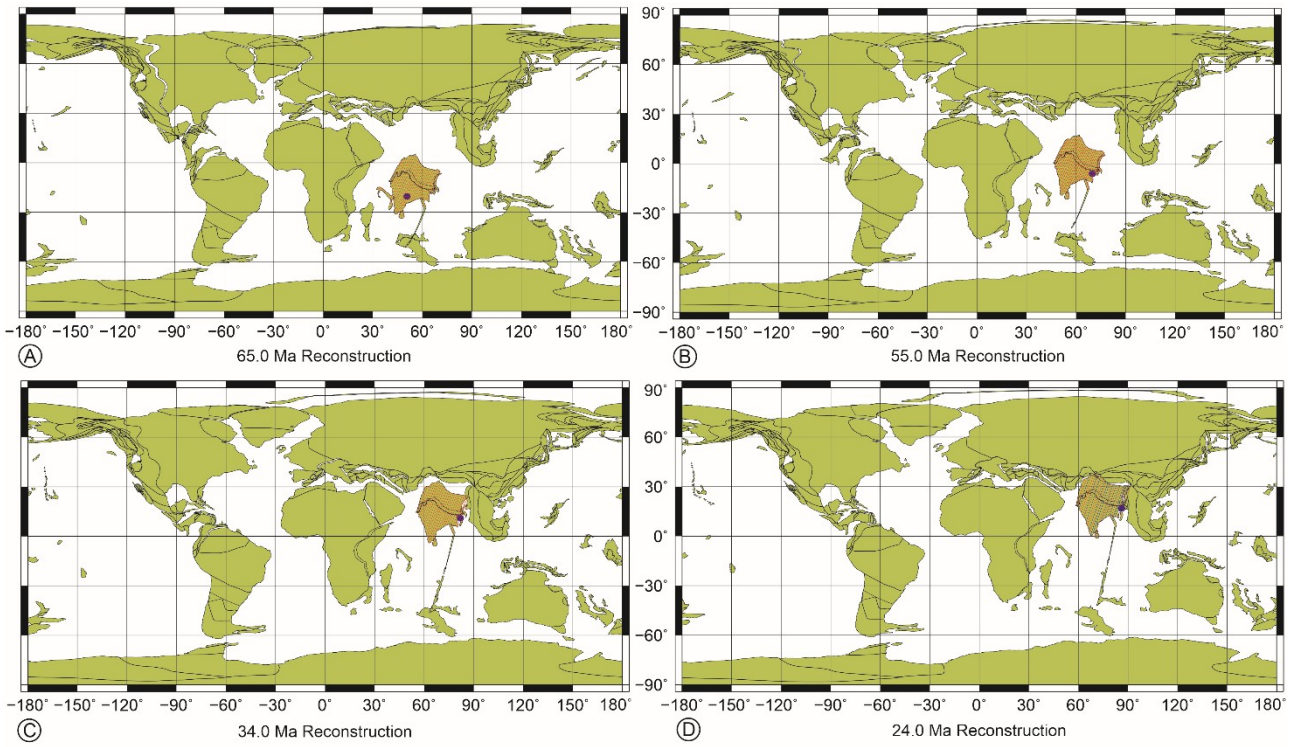

Fig. 1. Paleogeographic maps showing the latitudinal positions and monsoon regimes of India spanning from the Late Cretaceous to the Paleogene. (A) Reconstruction at 65 million years (Ma) showing the location of the Deccan Intertraps and a monsoon pattern akin to the I-AM (Indonesian–Australian Monsoon), indicated by red dotted lines. (B) Reconstruction at 55 Ma showing the location of Nongwalbibra, Meghalaya and a monsoon pattern similar to I-AM (indicated by red dotted lines). (C) Reconstruction at 34 Ma showing the location of Laisong, Nagaland and a monsoon pattern similar to I-AM (indicated by red dotted lines). (D) Reconstruction at 24 Ma showing the location of Makum, Assam and depicting a monsoon pattern showing similarities with both I-AM (red dotted lines) and SAM (South Asian Monsoon, shown by blue dotted lines). Maps prepared from ODSN Plate Tectonic Reconstruction Service (https://www.odsn.de/odsn/services/paleomap/paleomap.html).

tions by Mishra et al. (2022, 2024), using the Coexistence Approach (CA) on palynological data from the same and additional sites of late Maastrichtian age, also point to a humid climate with strong seasonality. They estimated a MAP of 189 ± 20.8 cm, with rainfall ranging from 33.5 ± 1.5 cm in the wettest month to 2.6 ± 0.7 cm in the driest month. The winter temperatures, inferred from their study, also indicate a warm climate with a mean of 18.5 ± 3.3 °C. Further support for these humid climatic conditions comes from geochemical analyses. Ghoshmaulik et al. (2023) utilized triple oxygen isotopes ($\delta^{18}O$–$\Delta'^{17}O$) data derived from fossil wood collected from the Mandla lobe, yielding MAP estimates ranging from 176 ± 20 to 186 ± 20 cm/year. These independent lines of evidence—from leaf physiognomy, pollen assemblages, and stable isotopes—collectively suggest a persistently high-rainfall, warm climate during the latest Cretaceous to early Paleocene in the Indian subcontinent. These quantitative reconstructions are further corroborated by qualitative palaeobotanical indicators, including palynological assemblages and plant megafossils (Lakhanpal and Dayal, 1962; Samant and Mohabey, 2009; Smith et al., 2015; Wheeler et al., 2017; Mishra et al., 2024; Thakre et al., 2024 and references therein), which reflect the presence of mesophytic to hygrophytic vegetation adapted to warm and seasonally wet conditions.

3 The late Paleocene to Eocene climate of India

The early to middle Paleogene was marked by a series of pronounced global warming episodes known as hyperthermal events, which offer valuable analogs for understanding Earth's climate response to elevated greenhouse gas levels. Among these, the Paleocene–Eocene Thermal Maximum (PETM, ∼56 Ma), Eocene Thermal Maximum 2 (ETM-2, ∼53.7 Ma), the Early Eocene Climatic Optimum (EECO, ∼52–49 Ma), and the Middle Eocene Climatic Optimum (MECO, ∼40 Ma) stand out as key intervals of significant climatic and biotic change (Zachos et al., 2008; McInerney and Wing, 2011). These events were driven by the rapid injection of large volumes of

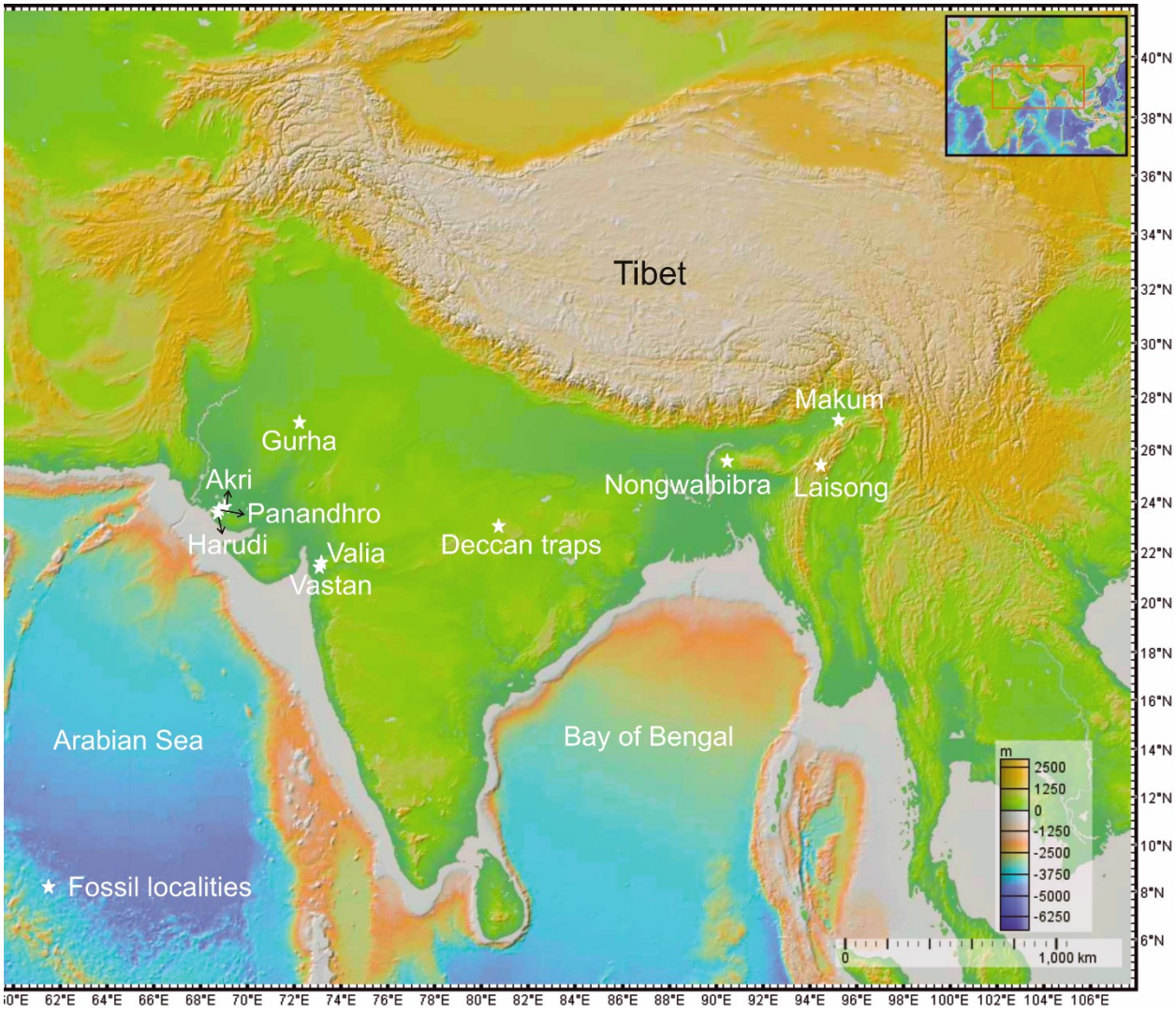

Fig. 2. Map showing fossil localities across various geological intervals: Deccan traps (Late Cretaceous–early Paleocene; Bhatia et al., 2021); Nongwalbibra (late Paleocene; Bhatia et al., 2021); Vastan and Valia (Paleocene Eocene Thermal Maximum; Samanta et al., 2013); Panandhro (Eocene Thermal Maximum-2; Srivastava et al., 2024); Akri and Gurha (Early Eocene Climatic Optimum; Shukla et al., 2014; Bhatia et al., 2021; Srivastava et al., 2023); Harudi (Middle Eocene Climatic Optimum; Deori et al., 2025); Laisong (late Eocene–early Oligocene; Bhatia et al., 2025) and Makum (late Oligocene; Srivastava et al., 2012; Bhatia et al., 2021).

^{12}C-enriched carbon into the atmosphere–ocean system, likely from volcanic activity, methane hydrate dissociation, or thermogenic processes (McInerney and Wing, 2011). This influx of carbon led to negative carbon isotope excursions (CIEs), ocean acidification, and global temperature rises, with atmospheric CO_2 concentrations exceeding 1000 ppm during several of these events (McInerney and Wing, 2011; Anagnostou et al., 2016; Harper et al., 2020). As a result, equator-to-pole temperature gradients decreased substantially, prompting poleward migration of tropical biota and widespread disruption of marine ecosystems (Wilf et al., 2003; Sluijs et al., 2009; Pross et al., 2012). The EECO, spanning approximately 52–49 Ma, represents the warmest and most prolonged greenhouse interval of the Cenozoic, with global mean annual temperatures estimated to be $\sim$13 $\pm$ 2.6 ℃ higher than today (Caballero and Huber, 2013). This sustained warmth had profound effects on terrestrial ecosystems, including major evolutionary radiations of mammals and angiosperms, significant floral turnover, and shifts in vegetation structure, particularly at mid- to high-latitudes (Wing et al., 1991; Woodburne et al., 2009; Agnini et al., 2014). In contrast, the MECO ($\sim$40 Ma) was a transient warming phase within a long-term cooling trend, lasting roughly 400–500 kyr.

Parameters	Deccan Inter-trappean (CLAMP)	Nongwalbibra (CLAMP)	Panandhro (CA)	Panandhro (CA)	Panandhro (CA)	Akri (CA)	Gurha (CLAMP)	Laisong (CLAMP)	Tirap (CLAMP)	SD (for CLAMP)
Modern coordinates	23.09° N; 80.62° E	25.4° N; 90.7° E	23.68° N; 68.76° E	23.68° N; 68.76° E	23.68° N; 68.76° E	23.6° N; 68.8° E	27.8° N; 72.8° E	25.5° N; 94.15° E	27.3° N; 95.7° E	–
Palaeo-coordinates	∼16° S	∼7.8° S	∼0.6° N	∼0.6° N	∼0.6° N	∼2.6° N	∼3.9° N	∼13.5° N	∼17° N	–
Age	K–Pg (∼66 Ma)	Late Paleocene (∼57–56 Ma)	Pre-Eocene Thermal Maximum-2 (Pre ETM-2) (∼53.7 Ma)	During ETM-2 (∼53.7 Ma)	After ETM-2 (∼53.7 Ma)	Early Eocene Climatic Optimum (EECO) (∼52–49 Ma)	Early Eocene (∼52–49 Ma)	Late Eocene–early Oligocene (∼33 Ma)	Late Oligocene (∼24–23 Ma)	–
MAT (℃)	23.4	22.2	26.6 (26 –27.3)	26.5 (26–27.1)	27.1 (26.5–27.7)	26.5 (26–27)	23.9	25.3	26	2.3
WMMT (℃)	28.1	27.5	27.6 (27.2–28.1)	27.1 (27.2–28.1)	27.9 (27.7–28.1)	27.6 (27.2–28)	28	28.9	28.4	2.9
CMMT (℃)	17.2	16.3	25.1 (24.3–25.9)	24.1 (24–24.1)	26 (25–27)	25.1 (24.3–25.9)	18.3	19.2	21.3	3.5
minTempW_1 (℃)	22.6	23	–	–	–	–	22.8	20.7	22.3	2.9
maxTempC_1 (℃)	22.8	22	–	–	–	–	24	25.2	27	3.5
RH.ann (%)	75.6	71	–	–	–	–	77.4	76.9	82.8	10.1
SH.ann (g kg^{-1})	13.8	12.6	–	–	–	–	14.5	14.9	16.2	1.8
ENTHALPY (kJ kg^{-1} x 10^{-1})	35	34.4	–	–	–	–	35.3	35.6	36.2	0.8
VPD.Ann (hPa)	6.8	7.6	–	–	–	–	8.1	7.8	8	2.3
VPD.Win (hPa)	6	5.8	–	–	–	–	6.8	6.8	7.3	1.5
VPD.Spr (hPa)	8.7	8.7	–	–	–	–	11.2	10.4	12.1	3.9
VPD.Sum (hPa)	5.4	8	–	–	–	–	6	5.4	4	3.4
VPD.Aut (hPa)	6.4	7.3	–	–	–	–	6.4	6.8	5.7	2

Table 1. CLAMP (Climate Leaf Analysis Multivariate Program) and CA (Coexistence Approach) reconstructed climate parameters for seven fossil assemblages from India spanning the Late Cretaceous–Paleogene (after Bhatia et al., 2021, 2025 and Srivastava et al., 2023, 2024).

Though less intense than the PETM or EECO, the MECO nonetheless resulted in a marked, globally synchronous temperature rise and carbon cycle disturbance (Bohaty and Zachos, 2003; Bohaty et al., 2009). Its origin remains less clearly understood, but it is thought to reflect complex interactions between tectonic, oceanographic, and carbon cycle processes (Bohaty and Zachos, 2003; Bohaty et al., 2009). Despite differences in duration and intensity, all these events underscore the sensitivity of Earth's climate and biosphere to carbon cycle perturbations and provide crucial insights into potential outcomes of ongoing anthropogenic climate change.

Attempts have been made to reconstruct the climate of the early Paleogene and these hyperthermal events (Samanta et al., 2013; Shukla et al., 2014; Bhatia et al., 2021; Srivastava et al., 2023, 2024; Deori et al., 2025) (Tables 1 and 2). Samanta et al. (2013) used high-resolution δ^{13}C stratigraphy, along with calcareous nannofossil, biomarker, and pollen data from the Cambay Shale lignite beds in western India (Fig. 2), to reveal a complete record of early Eocene CIEs, including the PETM, ETM-2 (H1/ELMO), H2, I1, and I2. The pronounced magnitude of these excursions suggests an intensified hydrological cycle during each hyperthermal. Proxy evidence from ∼56–52 Ma indicates that elevated tropical precipitation enhanced organic carbon burial and soil erosion, promoting thick lignite accumulation. Moreover, Srivastava et al. (2024) reconstructed the palaeoclimate across the pre-, peak-, and post-phases of the Eocene Thermal Maximum 2 using plant fossils from the paleo-equatorial region of western India (Tables 1 and 2), where atmospheric CO_2 exceeded 1000 ppmv. Estimated mean annual precipitation was 287.1 ± 55.9 cm before ETM2, dropped to 145.7 ± 8.0 cm during the event, and recovered to 265.1 ± 50.0 cm afterward. The results suggest that elevated CO_2 levels led to reduced rainfall and prolonged dry seasons, driving a

Parameters	Deccan Inter-trappean (CLAMP)	Nongwalbibra (CLAMP)	Panandhro (CA)	Panandhro (CA)	Panandhro (CA)	Akri (CA)	Gurha (CLAMP)	Laisong (CLAMP)	Tirap (CLAMP)	SD (for CLAMP)
Modern coordinates	23.09° N; 80.62° E	25.4° N; 90.7° E	23.68° N; 68.76° E	23.68° N; 68.76° E	23.68° N; 68.76° E	23.6° N; 68.8° E	27.8° N; 72.8° E	25.5° N; 94.15° E	27.3° N; 95.7° E	–
Palaeo-coordinates	~16° S	~7.8° S	~0.6° N	~0.6° N	~0.6° N	~2.6° N	~3.9° N	~13.5° N	~17° N	–
Age	K–Pg (~66 Ma)	Late Paleo-cene (~57–56 Ma)	Pre-Eocene Thermal Maximum-2 (Pre ETM-2) (~53.7 Ma)	During ETM-2 (~53.7 Ma)	After ETM-2 (~53.7 Ma)	Early Eocene Climatic Optimum (EECO) (~52–49 Ma)	Early Eocene (~52–49 Ma)	Late Eocene–early Oligocene (~33 Ma)	Late Oligocene (~24–23 Ma)	–
LGS	12.5	11.8	–	–	–	–	12.3	13.4	13.1	1.1
GSP (cm)	232	198.7	–	–	–	–	203.8	244.2	216.6	64.3
MAP (cm)			287.2 (259.2–315.1)	145.7 (137.7–153.7)	265.1 (221.1–315.1)	261.8 (259.2–264.5)	–	–	–	–
MMGSP (cm)	21.7	17.1	–	–	–	–	17.8	23.8	18.7	6.5
3WET (cm)	116.3	93.4	32.4 (25.9–38.9)	28.1 (25.9–30.3)	32.9 (27.0–38.9)	30.5 (27.0–34.0)	104	130.1	113.5	40
3DRY (cm)	23.7	18.7	10.1 (3.6–16.5)	4.85 (3.6–6.1)	13.4 (10.3–16.5)	5.9 (3.5–8.3)	11.3	21.7	9.9	9.8
MPwarm (cm)	–	–	21.4 (20.6–22.1)	13.4 (12.7–14.1)	17.8 (13.5–22.1)	21.3 (20.6–22.1)	–	–	–	–
growingD_2_div1000	103.7	96.3	–	–	–	–	105.4	114.8	116.1	11.6
growingD_3div1000	103.8	97.4	–	–	–	–	104.2	112.7	113	10.4
annualPE_1div10 (mm/year)	136	139.4	–	–	–	–	145.6	142.1	151.3	16.6
PETWarme_1 (mm/month)	129.8	146.9	–	–	–	–	139.4	128.2	133.5	24.5
PETColde_1 (mm/month)	78.2	80.7	–	–	–	–	96.9	91.6	113.4	14
3_WET:3_DRY	4.9	4.9	3.2	5.8	2.4	5.2	9.2	5.9	11.4	–

Table 2. CLAMP (Climate Leaf Analysis Multivariate Program) and CA (Coexistence Approach) reconstructed climate parameters for seven fossil assemblages from India spanning the Late Cretaceous–Paleogene (after Bhatia et al., 2021, 2025 and Srivastava et al., 2023, 2024).

shift from evergreen to deciduous forest dominance. Interestingly, Srivastava et al. (2023) have reconstructed the climate of EECO (Fig. 2) using the CA methodology on pollen assemblage (Tables 1 and 2) and suggested that the temperatures near the paleo-equator were higher compared to those at mid- and high latitudes. The presence of abundant rainfall likely improved plant water-use efficiency, helping vegetation remain resilient and functional despite the intense heat and elevated CO_2 levels during the EECO. Recently, Deori et al. (2025) have attempted to reconstruct the vegetation of MECO based on the pollen recovered from the Harudi Formation of Kutch, western India (Fig. 2), and inferred the significant presence of deciduous taxa during the main event, which shows an increase in the length of the dry season.

4 The late Eocene to early Oligocene climate of India

The shift from the late Eocene to the early Oligocene (~38 to 28 million years ago) represents a pivotal climatic transition in the Cenozoic Era, marked by a pronounced global cooling event (Zachos et al., 2001; Hönisch et al., 2023). This interval witnessed the Earth's progression from a warm, greenhouse climate to a cooler icehouse state, culminating in the formation of permanent ice sheets on Antarctica. In the late Eocene, the climate remained warm and humid, with subtropical and tropical vegetation extending into higher latitudes. However, tectonic changes—such as the opening of the Drake Passage and Tasmanian Gateway—progressively isolated Antarctica, allowing the Antarctic Circumpolar Current to develop (Hodel et al., 2021). Concurrently, atmospheric CO_2 levels declined below a critical threshold, promoting the rapid expansion of the Antarctic ice sheet and causing a notable drop in sea level. These climatic changes had far-reaching ecological consequences, including widespread faunal turnovers, shifts in vegetation patterns, and increased aridification across interior regions of continents, especially in Asia and Africa. Bhatia et al. (2025) have reconstructed the climate of the late Eocene–early Oligocene (Tables 1 and 2) based on the fossil leaf morphological traits recovered from the Laisong Formation of northeast India (Fig. 2). They suggested that a warm and humid climate with seasonal rainfall was present during the deposition of the Laisong Formation sediments.

5 The late Oligocene climate of India

Pälike et al. (2006) present a 13-million-year high-resolution climate record from the equatorial Pacific (ODP Site 1218), revealing a distinct "heartbeat" of the Oligocene climate system driven by Earth's orbital variations. They identify strong 405,000-year eccentricity cycles in the global carbon cycle and 1.2-million-year obliquity modulations associated with recurring glacial events. Two major glaciation events—Oi-1 (at ∼33.9 Ma) and Mi-1 (at ∼23 Ma)—mark the beginning and end of the Oligocene, with a significant mid-Oligocene cold phase in between. The study's climate-carbon modeling shows that orbital forcing, especially eccentricity and obliquity, strongly influenced ocean carbon storage, productivity, and deep-sea chemistry, highlighting a tightly coupled interaction between solar insolation, ice volume, and the carbon cycle in Earth's early icehouse climate. The terrestrial climate record for the late Oligocene remains limited due to sparse data availability. However, efforts have been made to reconstruct the paleoclimate of this period using quantitative methods. Notably, Srivastava et al. (2012) and Bhatia et al. (2021) conducted climate reconstructions (Tables 1 and 2) based on fossil leaf morphological traits collected from the Tikak Parbat Formation in the Makum Coalfield, Assam, in northeast India (Fig. 2). Their analyses, employing leaf physiognomy techniques, indicate that the region experienced a warm and humid climate during the late Oligocene. The estimated cold-month mean temperature exceeded 20 ℃, suggesting the absence of a true winter season. Additionally, the reconstructions reveal strong rainfall seasonality, pointing to a monsoonal climate regime characterized by a pronounced wet and dry season. These findings provide valuable insights into the terrestrial climate dynamics of South Asia during a time of significant global climatic transition.

6 Synthesis

Globally, the Paleogene was characterized by a significantly warmer climate compared to the Neogene. This interval was punctuated by several short-lived but extreme global warming events, commonly referred to as hyperthermals, including the Paleocene–Eocene Thermal Maximum (PETM), Eocene Thermal Maximum 2 (ETM-2), the Early Eocene Climatic Optimum (EECO), and the Middle Eocene Climatic Optimum (MECO) (Zachos et al., 2001; Hönisch et al., 2023). These hyperthermal events represent transient episodes of intensified greenhouse conditions, superimposed on an already warm background climate. The primary driver of this sustained warmth during the Paleogene was elevated atmospheric carbon dioxide (CO_2) concentrations. Although CO_2 levels generally declined over the course of the Paleogene, they remained substantially higher than in subsequent epochs, and episodic increases were associated with the aforementioned hyperthermal events (Hönisch et al., 2023).

A comparison with the earlier Maastrichtian warming phase—occurring during the Late Cretaceous—reveals notable differences in both the causes and mechanisms of greenhouse gas emissions. During the Maastrichtian, large-scale volcanic activity, particularly from the Deccan Traps, is considered the dominant source of atmospheric CO_2 increase, which contributed to global warming during that time (Westerhold et al., 2025). In contrast, the Paleogene hyperthermals appear to have been driven by a more diverse and complex array of carbon sources. These include the destabilization of methane clathrates, widespread wildfires, thermogenic methane released from organic-rich sediments, the drying of epicontinental seas, and thawing permafrost (Dickens et al., 1997; Katz et al., 2001; Gavrilov et al., 2003; Kent et al., 2003; Svensen et al., 2004; DeConto et al., 2012). These processes released massive quantities of greenhouse gases into the atmosphere over relatively short geological timescales. Many of these carbon release events were likely triggered or modulated by orbital (astronomical) forcing, which affected Earth's insolation patterns and subsequently influenced climate feedbacks and carbon cycle dynamics.

Bhatia et al. (2021) have analyzed leaf morphological traits (Fig. 3) recovered from the Late Cretaceous to Paleogene sediments of India, investigating how the Indian monsoon system evolved in response to the Indian plate's long northward drift following its separation from Gondwana. Over a period of about 160 million years, the Indian plate travelled roughly 9000 km across the tropics, experiencing a range of climatic conditions due to both its changing latitude and global climate fluctuations. Their results show that, from the Late Cretaceous to the Eocene, India experienced a persistent monsoonal climate akin to the present-day Indonesian–Australian Monsoon (I-AM) (Fig. 4A–C), driven by seasonal migrations of the Intertropical Convergence Zone (ITCZ). This system differed markedly from the modern South Asian Monsoon (SAM), which is strongly influenced by the orographic barrier of the Himalaya—a feature that only emerged significantly later in the Neogene. The fossil leaf traits revealed that, although monsoonal conditions were present from the Late Cretaceous onward, features associated with the modern monsoon did not appear until the late Oligocene (Fig. 4A–C). This suggests that the modern SAM developed relatively recently in Earth's history, likely in response to the uplift of the Himalaya.

During the Paleogene, the ITCZ appears to have migrated over a wider latitudinal range than today, leading to seasonally variable but non-extreme equatorial climates. Despite being part of a globally warm ("hyperthermal") period, the reconstructed terrestrial temperatures in India were warm but not excessively hot, possibly moderated by

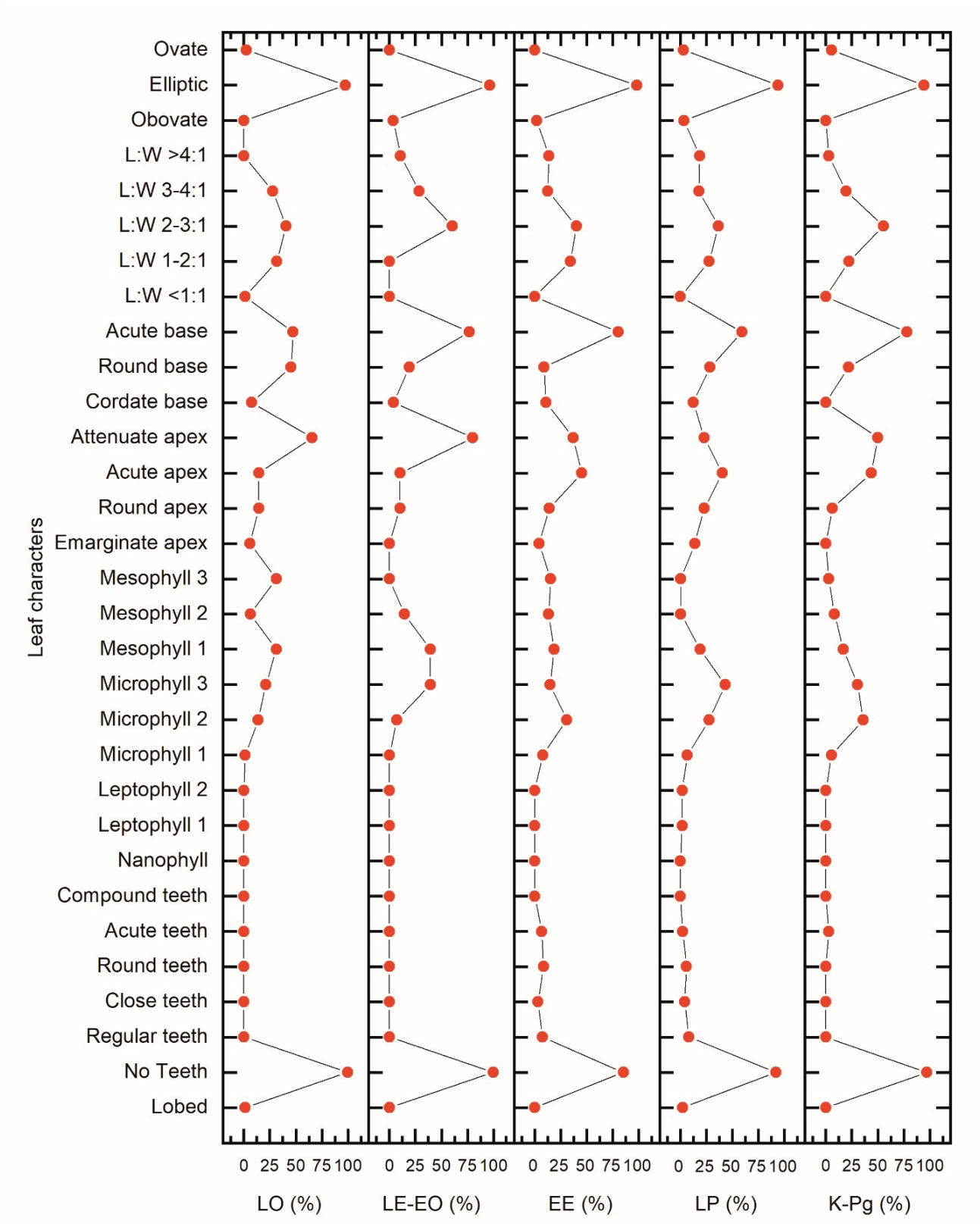

Fig. 3. Diagram showing the percentage of 31 leaf morphological traits used in the CLAMP analysis across different geological ages: LO (late Oligocene; Bhatia et al., 2021), LE–EO (late Eocene–early Oligocene; Bhatia et al., 2025), EE (early Eocene; Bhatia et al., 2021), LP (late Paleocene; Bhatia et al., 2021), and K–Pg (Late Cretaceous–early Paleocene; Bhatia et al., 2021).

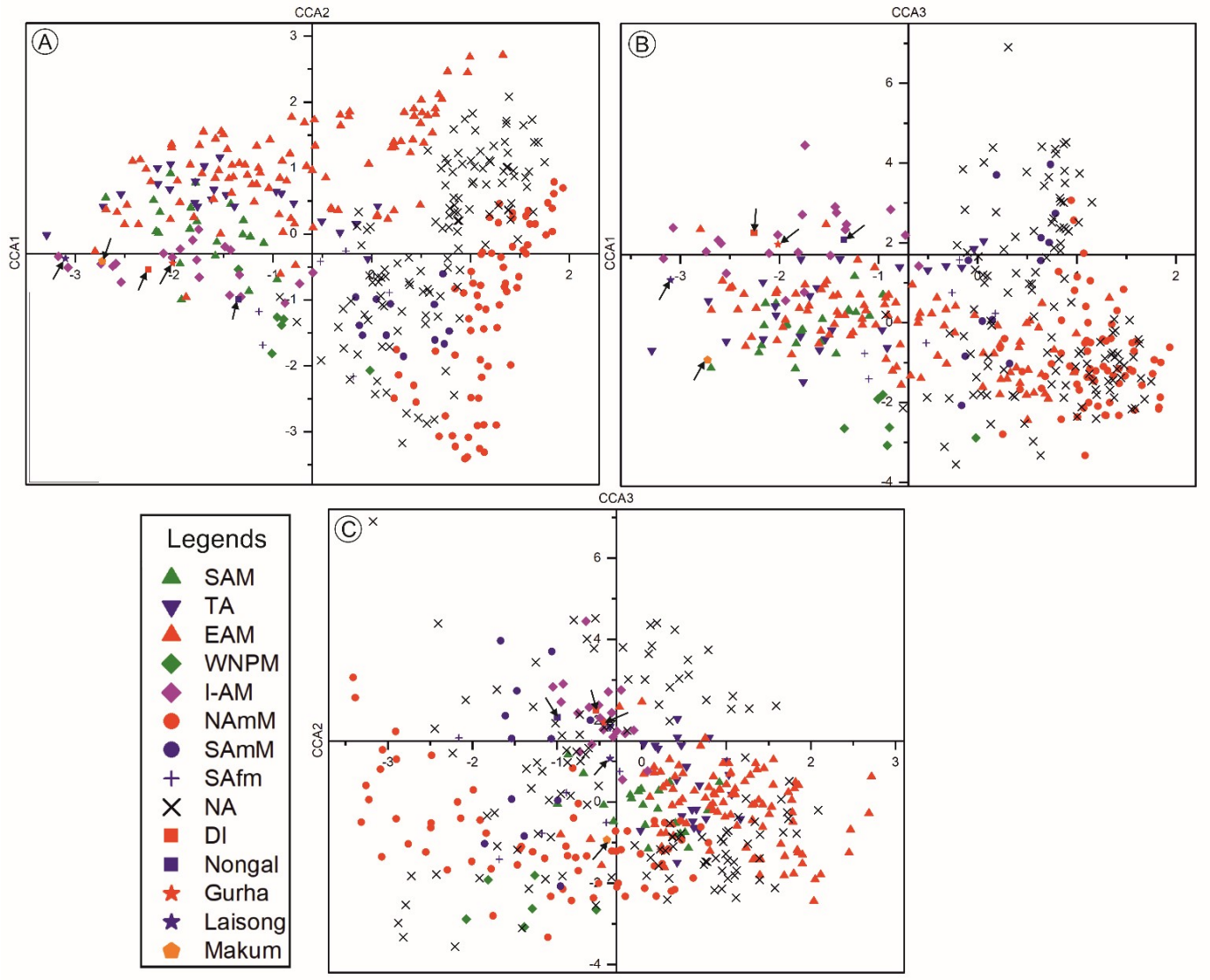

Fig. 4. Figure showing CCA1–3 plots of modern and fossil leaf morphological traits. (A–C) CCA plot showing positions of the modern and fossil forests in the physiognomic space. Individual forest sites are coded for their leaf trait adaptations to the South Asia Monsoon (SAM), Transition Area (TA), East Asia Monsoon (EAM), Western North Pacific Monsoon (WNPM), Indonesian–Australian Monsoon (I-AM), North American Monsoon (NAmM), South American Monsoon (SAmM), South African Monsoon (SAfm) and no monsoon (NM) climates along with the fossil localities. All the fossil sites, Deccan traps (DI), Nongwalbibra (Nongal), Gurha, Laisong and Makum are positioned passively in the physiognomic space (after Bhatia et al., 2021, 2025).

regional elevation or climatic mechanisms not present today. In terms of precipitation, all sites showed high annual rainfall, generally exceeding 190 cm, but with clear seasonality (Fig. 5A–I, Fig. 6A–I). Early assemblages like those from the Deccan Intertrappean and Nongwalbibra showed more uniform rainfall patterns, whereas younger sites such as Gurha and Tirap displayed strong seasonal contrasts (Fig. 5A–I, Fig. 6A–I), with much higher precipitation during the wettest months compared to the driest—ratios consistent with monsoonal climates. Overall, this research demonstrates that India experienced a consistent monsoonal climate throughout its passage across the tropics, but that the dominant monsoon system resembled the I-AM rather than the SAM. The SAM likely arose after India's collision with Asia and the subsequent Himalayan uplift.

Recently, Bhatia et al. (2025) reconstructed the climate of the late Eocene–early Oligocene based on fossil leaf morphological traits (Fig. 3) recovered from the Laisong Formation sediments (Tables 1 and 2). By comparing the

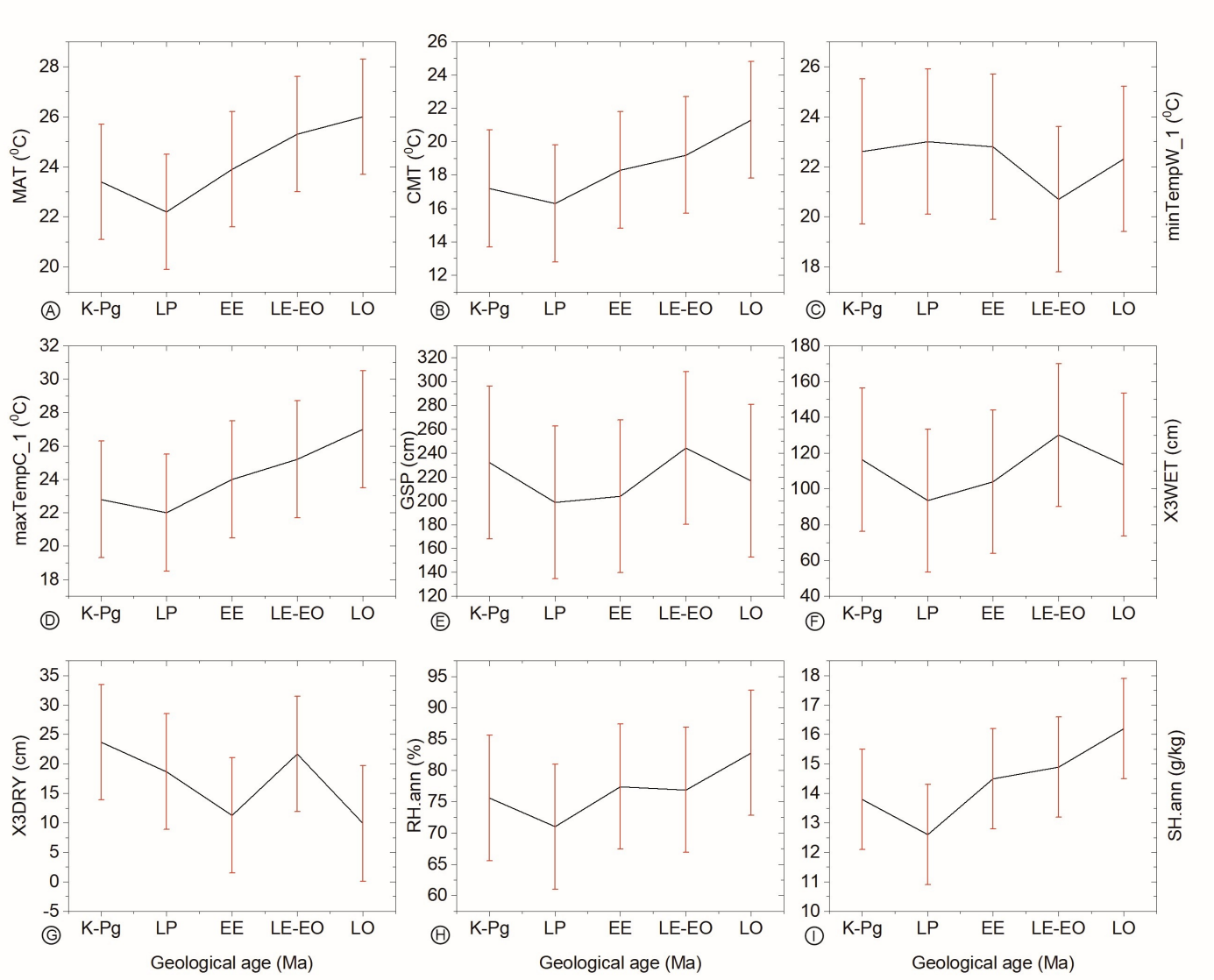

Fig. 5. Graphs showing various climatic parameters obtained from CLAMP analysis across different geological ages; K–Pg (Late Cretaceous–early Paleocene), LP (late Paleocene), EE (early Eocene), LE–EO (late Eocene–early Oligocene) and LO (late Oligocene) (after Bhatia et al., 2021, 2025). (A) Mean Annual Temperature (MAT) (℃). (B) Cold Month Mean Temperature (CMT) (℃). (C) Minimum temperature of the warmest month (minTempW_1) (℃). (D) Maximum temperature of the coldest month (maxTempC_1) (℃). (E) Growing Season Precipitation (GSP) (cm). (F) Precipitation during the three wettest months (X3WET) (cm). (G) Precipitation during the three driest months (X3DRY) (cm). (H) Relative humidity (RH.ann) (%). (I) Specific humidity (SH.ann) (g kg^{-1}).

rainfall patterns with previously reconstructed data spanning from the Late Cretaceous to the Paleogene (Bhatia et al., 2021), they suggested that the late Eocene–early Oligocene experienced exceptionally high rainfall (Figs. 5, 6). This is an important finding, as it highlights the role of regional and local factors—such as paleogeography and proximity to moisture sources—in shaping climate responses. During this time, northeast India was located near the equator and close to the paleo–Bay of Bengal, which likely provided abundant atmospheric moisture and helped maintain a humid environment. Its tropical position also contributed to sustained warmth. These results show why region-specific climate reconstructions are essential to fully understand the spatial variability during major climatic transitions.

Interestingly, reconstructions based on vegetation analysis during two major Paleogene hyperthermal events—the Eocene Thermal Maximum 2 (ETM-2) and the Middle

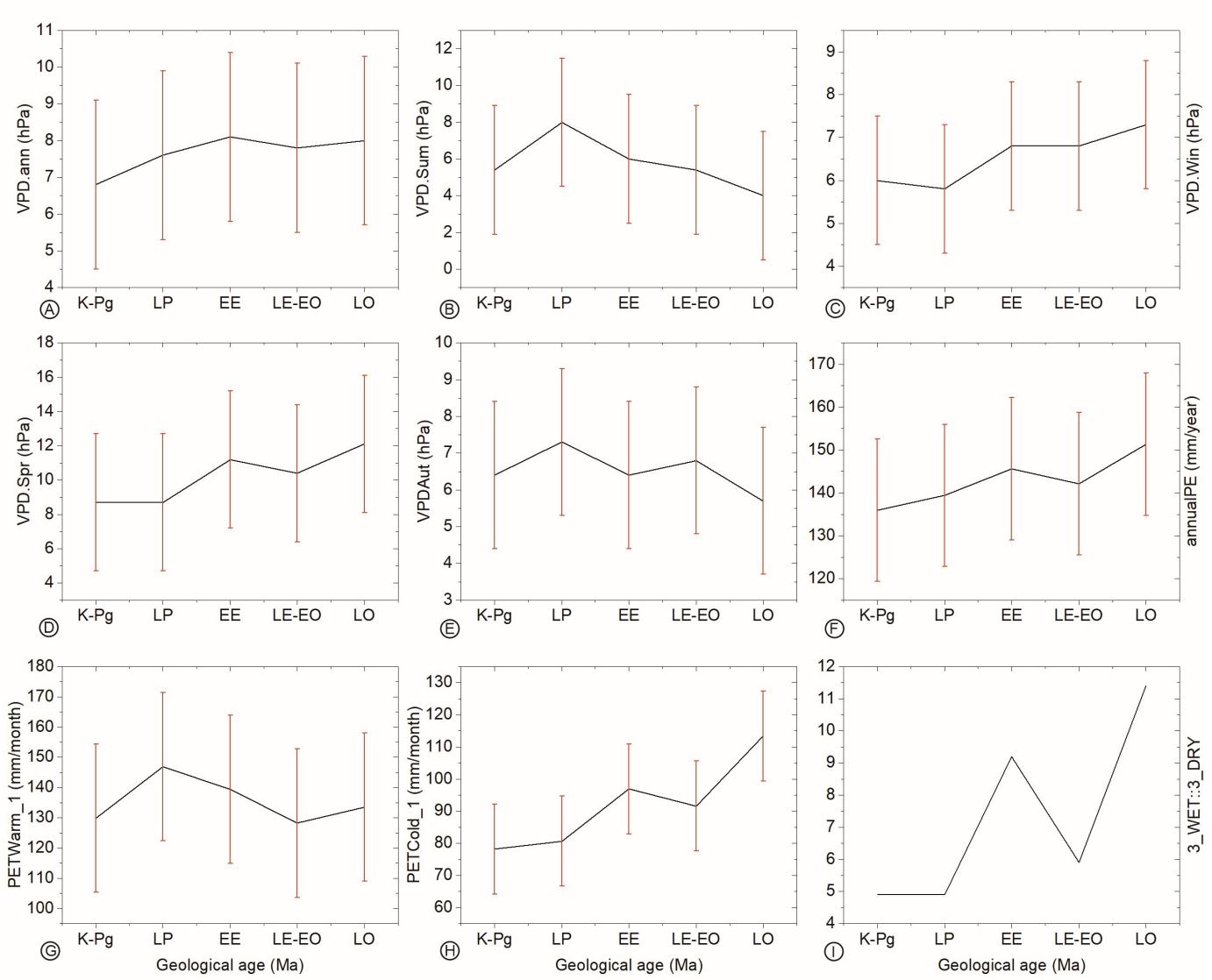

Fig. 6. Graphs showing various climatic parameters obtained from CLAMP analysis across different geological ages; K–Pg (Late Cretaceous–early Paleocene), LP (late Paleocene), EE (early Eocene), LE–EO (late Eocene–early Oligocene) and LO (late Oligocene) (after Bhatia et al., 2021, 2025). (A) Mean annual vapour pressure deficit (VPD.Ann) (hPa). (B) Mean summer vapour pressure deficit (VPD.Sum) (hPa). (C) Mean winter vapour pressure deficit (VPD.Win) (hPa). (D) Mean spring vapour pressure deficit (VPD.Spr) (hPa). (E) Mean autumn vapour pressure deficit (VPD.Aut) (hPa). (F) Mean Annual Potential evapotranspiration (annualPE) (mm/year). (G) Mean monthly PET of the warmest quarter (PETWarm_1) (mm/month). (H) Mean monthly PET of the coldest quarter (PETCold_1) (mm/month). (I) Ratio of Precipitation during the three wettest months to Precipitation during the three driest months (3_WET:3_DRY).

Eocene Climatic Optimum (MECO)—by Srivastava et al. (2024) and Deori et al. (2025), respectively, suggest a notable increase in deciduous plant taxa. Indian ecosystems, situated near the paleo-equator, responded differently than those at higher latitudes. While global data often indicate increased productivity and diversity during hyperthermal, Indian floras reflect a more stress-prone adaptation. The dominance of drought-deciduous and disturbance-adapted taxa suggests ecological restructuring in response to prolonged dry seasons. This is supported by the decline of evergreen taxa during ETM-2 and MECO, indicating intensified seasonality despite warming trends. In contrast, the climate during the Early Eocene Climatic Optimum (EECO)—recognized as the longest sustained warm interval of the Eocene—was characterized by warm and humid conditions with consistently high rainfall. These favor-

able conditions supported the long-term stability of evergreen tropical rainforests (Srivastava et al., 2023), minimizing seasonal water stress and promoting vegetational resilience. The abundant and relatively stable moisture availability during this time likely minimized seasonal water stress, allowing evergreen tropical vegetation to flourish. This contrast between short-lived hyperthermal and the stable EECO regime provided a stable climatic regime conducive to the long-term maintenance of dense, diverse rainforest ecosystems and highlights the complex interplay of warming, hydrology, and vegetation dynamics.

Notably, palynological data from hyperthermal intervals such as the PETM, ETM-2, and MECO reveal an increased abundance of drought-deciduous and disturbance-tolerant taxa. These shifts reflect substantial restructuring of vegetation communities in response to intensified seasonality and hydrological stress. However, the persistence of key floristic lineages across these warming phases suggests a notable degree of ecological resilience in tropical, low-latitude regions such as India. As reported by Srivastava et al. (2024), prior to ETM-2, evergreen taxa accounted for 83% of the flora, while deciduous types comprised only 3%. During the peak of warming, the proportion of deciduous taxa quadrupled to 12%, while evergreen species declined to 74%. Moisture-loving plants such as palms and pteridophytes declined, whereas drought-tolerant legumes became more prominent. Following the ETM-2 event, evergreen taxa rebounded, indicating that the forest ecosystem oscillated in composition in response to climatic stress. Rather than widespread extinctions, the fossil evidence points to adaptive turnover and ecosystem reassembly, likely driven by life-history shifts such as transitions from evergreen to deciduous growth strategies. Complementary evidence from the EECO fossil record (Srivastava et al., 2023) further suggests that persistently high rainfall near the palaeo-equator may have enhanced the resilience of tropical rainforests by improving the water-use efficiency of vegetation under greenhouse conditions. Collectively, these patterns underscore the dynamic and responsive nature of vegetation to transient climatic stress and highlight the value of the Indian fossil record for understanding both the vulnerability and resilience of tropical ecosystems during abrupt and sustained warming episodes of the Paleogene.

Beyond floristic responses, limited evidence exists for broader biotic changes during Paleogene hyperthermal events in the Indian subcontinent. Vertebrate records from the Cambay Shale, particularly the Vastan lignite mine, suggest possible faunal exchange during the ETM-2, likely facilitated by climate-driven dispersal (Clementz et al., 2011). Marine foraminiferal records from the Kutch Basin provide valuable insights into the ecological impacts of these events. Low-diversity, dwarf foraminifera and eutrophic indicators dominated during the PETM and ETM-2, whereas the EECO and MECO were associated with more stable, oligotrophic conditions that supported high diversity and the development of carbonate platforms (Khanolkar and Saraswati, 2019). These trends suggest that, despite episodes of transient environmental stress, shallow marine ecosystems in western India exhibited notable resilience throughout much of the Eocene (Khanolkar and Saraswati, 2019). Although soil microbial proxies remain unexplored in the Indian Paleogene, their proven utility in other regions highlights their strong potential for future research. Integrating faunal and microbial evidence with palaeobotanical data would substantially improve our understanding of ecosystem-wide responses to early Cenozoic climate perturbations in tropical regions.

While these findings offer valuable regional perspectives, they are limited by the spatial concentration of available fossil data. Most records originate from central, western, and northeastern India, with southern and central-eastern regions underrepresented. This bias results from uneven preservation and exploration of plant fossil sites across the subcontinent. To achieve a more comprehensive understanding of paleoclimate variability, future studies should focus on generating high-resolution, multi-proxy datasets from these underexplored regions, especially southern India.

7 Conclusion

The northward journey of the Indian plate from Gondwana to its eventual collision with Asia was a remarkable geological and climatic event, significantly influencing the subcontinent's environmental history. This tectonic voyage was accompanied by substantial climatic fluctuations and vegetation shifts, largely driven by variations in atmospheric carbon dioxide levels released from multiple natural sources, and modulated by astronomical (orbital) forcing. In the Indian context, palaeovegetation and climatic reconstructions from the Late Cretaceous to the Paleogene reveal pronounced changes in the monsoonal intensity and hydrological cycle, closely linked to fluctuations in CO_2 concentrations and seasonal insolation patterns. These variations not only shaped the evolution and distribution of plant communities across the Indian subcontinent but also provide critical insights into how global climate drivers operated in low-latitude regions like India during periods of intense climatic and tectonic transformation. Observed responses during hyperthermal provide valuable analogs for understanding present-day hydrological extremes under global warming. To deepen this understanding, future research should focus on high-resolution, multi-proxy records, particularly from underrepresented regions like southern India, to better resolve spatial climate gradients and improve predictions of ecosystem responses to ongoing climate change.

Acknowledgments

The authors are grateful to the Director of the Birbal Sahni Institute of Palaeosciences, Lucknow for providing necessary facilities and encouragement during the research work. The authors express their gratitude to Prof. Robert Spicer (Open University, UK), Prof. Jian Yang (Institute of Botany, Chinese Academy of Sciences), and numerous other collaborators for their significant contributions to the development and upkeep of CLAMP, as well as for providing free access to its website (http://clamp.ibcas.ac.cn/CLAMP_Online.html). The authors also thank Prof. M. Santosh for his invitation to contribute this paper to Habitable Planet. We are also grateful to him for his valuable suggestions that helped improve the manuscript. The authors also express their gratitude to Prof. Cheng-Xue Yang (Editor-in-Chief) and the two anonymous reviewers, for their valuable suggestions, which have significantly enhanced the manuscript.

Declaration of competing interest

The authors declare that he has no known competing financial interests or personal relationships that could have appeared to influence the work reported in this paper.

Credit Author statement

Gaurav Srivastava: Conceptualization; Investigation; Visualization; Writing—original draft; Writing—review & editing.

Harshita Bhatia: Investigation; Writing—review & editing.

References

Agnini, C., Fornaciari, E., Raffi, I., Catanzariti, R., Pälike, H., Backman, J., Rio, D., 2014. Biozonation and biochronology of Paleogene calcareous nannofossils from low and middle latitudes. Newsl. Stratigr. 47, 131–181. doi:10.1127/0078-0421/2014/0042.

Anagnostou, E., John, E.H., Edgar, K.M., Foster, G.L., Ridgwell, A., Inglis, G.N. et al., 2016. Changing atmospheric CO_2 concentration was the primary driver of early Cenozoic climate. Nature 533, 380–384. doi:10.1038/nature17423.

Bhatia, H., Khan, M.A., Srivastava, G. et al., 2021. Late Cretaceous–Paleogene Indian monsoon climate vis-a-vis movement of the Indian plate, and the birth of the South Asian Monsoon. Gondwana Res. 93, 89–100. doi:10.1016/j.gr.2021.01.010.

Bhatia, H., Lokho, K., Srivastava, G., Ezung, O.C., 2025. Quantifying the equatorial climate shifts in the Indo-Burma range using late Eocene–early Oligocene leaf fossils. Palaeogeogr. Palaeoclimatol. Palaeoecol. 669, 112931. doi:10.1016/j.palaeo.2025.112931.

Bohaty, S.M., Zachos, J.C., 2003. Significant Southern Ocean warming event in the late middle Eocene. Geology 31, 1017–1020. doi:10.1130/G19800.1.

Bohaty, S.M., Zachos, J.C., Florindo, F., Delaney, M.L., 2009. Coupled greenhouse warming and deep-sea acidification in the middle Eocene. Paleoceanogr. Paleoclimatol. 24, PA2207. doi:10.1029/2008PA001676.

Bossuyt, F., Milinkovitch, M.C., 2001. Amphibians as Indicators of Early Tertiary "Out-of-India" dispersal of vertebrates. Science 292, 93–95. doi:10.1126/science.1058875.

Caballero, R., Huber, M., 2013. State-dependent climate sensitivity in past climates and its implications for future climate projections. Proc. Natl. Acad. Sci. USA 110, 14162–14167. doi:10.1073/pnas.130336511.

Chatterjee, S., Goswami, A., Scotese, C.R., 2013. The longest voyage: tectonic, magmatic, and palaeoclimatic evolution of the Indian plate during its northward flight from Gondwana to Asia. Gondwana Res. 23, 238–267. doi:10.1016/j.gr.2012.07.001.

Clementz, M., Bajpai, S., Ravikant, V., Thewissen, J.G.M., Saravanan, N., Singh, I.B., Prasad, V., 2011. Early Eocene warming events and the timing of terrestrial faunal exchange between India and Asia. Geology 39(1), 15–18. doi:10.1130/G31585.1.

DeConto, R.M., Galeotti, S., Pagani, M., Tracy, D. et al., 2012. Past extreme warming events linked to massive carbon release from thawing permafrost. Nature 484(7392), 87–91. doi:10.1038/nature10929.

Deori, N., Verma, P., Agrawal, S., Thakkar, M.G., Patel, J.M., 2025. Response of tropical rainforest to warming during Middle Eocene Climate Optimum (MECO): evidence from palynological record from the Bartonian deposits of Kutch Basin, Western India. Evol. Earth 3, 100065. doi:10.1016/j.eve.2025.100065.

Dickens, G.R., Castillo, M.M., Walker, J.C.G, 1997. A blast of gas in the latest Paleocene: simulating first-order effects of massive dissociation of oceanic methane hydrate. Geology 25, 259–262. doi:10.1130/0091-7613.

Gavrilov, Y.O., Shcherbinina, E.A., Oberhänsli, H., 2003. Paleocene-Eocene boundary events in the northeastern Peri-Tethys. Geol. Soc. Am. Spec. Pap. 369, 147–168. doi:10.1130/0-8137-2369-8.147.

Ghoshmaulik, S., Bhattacharya, S.K., Hazra, M., Roy, P., Khan, M.A. et al., 2023. Triple oxygen isotopes in intertrappean fossil woods: evidence of higher tropical rainfall during Deccan volcanism. Chem. Geol. 634, 121599. doi:10.1016/j.chemgeo.2023.121599.

Harper, D.T., Honisch, B., Zeebe, R.E., Shaffer, G., Haynes, L.L., Thomas, H.E., Zachos, J.C., 2020. The magnitude of surface ocean acidification and carbon release during Eocene thermal Maximum 2 (ETM2) and the Paleocene Eocene thermal Maximum (PETM). Paleoceanogr. Paleoclimatol. 35, e2019PA003699. doi:10.1029/2019PA003699.

Held, I.M., Soden, B.J., 2006. Robust responses of the hydrological cycle to global warming. J. Clim. 19, 5686–5699. doi:10.1175/JCLI3990.1.

Hodel, F., Grespan, R., de Rafélis, M., Dera, G., Lezin, C. et al., 2021. Drake Passage gateway opening and Antarctic Circumpolar Current onset 31 Ma ago: the message of foraminifera and reconsideration of the Neodymium isotope record. Chem. Geol. 570, 120171. doi:10.1016/j.chemgeo.2021.120171.

Hönisch et al., 2023. (The Cenozoic CO_2 Proxy Integration Project ($CenCO_2PIP$) Consortium). Toward a Cenozoic history of atmospheric CO_2. Science 382, eadi5177. doi:10.1126/science.adi5177.

Jay, A.E., Widdowson, M., 2008. Stratigraphy, structure and volcanology of the SE Deccan continental flood basalt province: implications for eruptive extent and volumes. J. Geol. Soc. Lond. 165, 177–188. doi:10.1144/0016-76492006-062.

Kale, V.S., 2020. Cretaceous volcanism in peninsular India: Rajmahal-Sylhet and Deccan Traps, in: Gupta, N., Tandon, S.K. (Eds.), Geodynamics of the Indian Plate. Springer International Publishing, Switzerland. doi:10.1007/978-3-030-15989-4_8.

Kapur, V.V., Khosla, A., 2018. Faunal elements from the Deccan volcanosedimentary sequences of India: a reappraisal of biostratigraphic, palaeoecological, and palaeobiogeographic aspects. Geol. J. 54, 2797–2828. doi:10.1002/gj.3379.

Katz, M.E., Cramer, B.S., Mountain, G.S., Katz, S., Miller, K.G., 2001. Uncorking the bottle: what triggered the Paleocene/Eocene thermal maximum methane release? Paleoceanography 16, 549–562. doi:10.1029/2000PA000615.

Kent, D.V., Cramer, B.S., Lanci, L., Wang, D., Wright, J.D., Vander Voo, R., 2003. A case for a comet impact trigger for the Paleocene/Eocene thermal maximum and carbon isotope excursion. Earth Planet. Sci. Lett. 211(1), 13–26. doi:10.1016/S0012-821X(03)00188-2.

Khanolkar, S., Saraswati, P.K., 2019. Eocene foraminiferal biofacies in

Kutch Basin (India) in context of palaeoclimate and palaeoecology. J. Palaeogeogr. 8, 21. doi:10.1186/s42501-019-0038-2.

Lakhanpal, R.N., Dayal, R., 1962. *Mallotoxylon keriense* gen. et sp. nov., a fossil dicotyledonous wood from the Deccan Intertrappean Series. India. J. Paleosci. 11, 149–153. doi:10.54991/jop.1962.635.

McInerney, F.A., Wing, S.L., 2011. The Paleocene-Eocene Thermal Maximum: a perturbation of carbon cycle, climate, and biosphere with implications for the future. Annu. Rev. Earth Planet. Sci. 39, 489–516. doi:10.1146/annurev-earth-040610-133431.

Mishra, S., Bansal, M., Prasad, V., Singh, V.P., Murthy, S., Parmar, S. et al., 2024. Did the Deccan Volcanism impact the Indian flora during the Maastrichtian? Earth Sci. Rev. 258, 104950. doi:10.1016/j.earscirev.2024.104950.

Mishra, S., Singh, S.P., Arif, M., Singh, A.K., Srivastava, G., Ramesh, B.R., Prasad, V., 2022. Late Maastrichtian vegetation and palaeoclimate: palynological inferences from the Deccan Volcanic Province of India. Cretac. Res. 133, 105–126. doi:10.1016/j.cretres.2021.105126.

Osman, M.B., Tierney, J.E., Zhu, J., Tardif, R., Hakim, G.J., King, J., Poulsen, C.J., 2021. Globally resolved surface temperatures since the Last Glacial Maximum. Nature 599, 239–244. doi:10.1038/s41586-021-03984-4.

Pälike, H., Norris, R.D., Herrle, J.O., Wilson, P.A., Coxall, H.K., Lear, C.H., Shackleton, N.J., Tripati, A.K., Wade, B.S., 2006. The heartbeat of the Oligocene climate system. Science 314(5807), 1894–1898. doi:10.1126/science.1133822.

Pierrehumbert, R.T., 2002. The hydrologic cycle in deep-time climate problems. Nature 419, 191–198. doi:10.1038/nature01088.

Pross, J., Contreras, L., Bijl, P.K., Greenwood, D.R., Bohaty, S.M., Schouten, S., Bendle, J.A., Rohl, U., 2012. Persistent near-tropical warmth on the Antarctic continent during the early Eocene epoch. Nature 488, 73–77. doi:10.1038/nature11300.

Pusok, A.E., Stegman, D.R., 2020. The convergence history of India-Eurasia records multiple subduction dynamics processes. Sci. Adv. 6(19), eaaz8681. doi:10.1126/sciadv.aaz8681.

Rose, K., Holbrook, L., Rana, R. et al., 2014. Early Eocene fossils suggest that the mammalian order Perissodactyla originated in India. Nature Commun. 5, 5570. doi:10.1038/ncomms6570.

Samant, B., Mohabey, D.M., 2009. Palynoflora from Deccan volcanosedimentary sequence (Cretaceous-Palaeogene transition) of central India: implications for spatio-temporal correlation. J. Biosci. 34, 811–823. doi:10.1007/s12038-009-0064-9.

Samanta, A., Bera, M.K., Ghosh, R., Bera, S., Filley, T., Pande, K., Rathore, S.S., Rai, J., Sarkar, A., 2013. Do the large carbon isotopic excursions in terrestrial organic matter across Paleocene–Eocene boundary in India indicate intensification of tropical precipitation? Palaeogeogr. Palaeoclimatol. Palaeoecol. 387, 91–103. doi:10.1016/j.palaeo.2013.07.008.

Shukla, A., Mehrotra, R.C., Spicer, R.A., Spicer, T.E.V., Kumar, M., 2014. Cool equatorial terrestrial temperatures and the South Asian monsoon in the Early Eocene: evidence from the Gurha Mine, Rajasthan, India. Palaeogeogr. Palaeoclimatol. Palaeoecol. 412, 187–198. doi:10.1016/j.palaeo.2014.08.004.

Sluijs, A., Schouten, S., Donders, T.H., Schoon, P.L., Röhl, U., Reichart, G.J., Sangiorgi, F., Kim, J.H., Damsté, J.S.S., Brinkhuis, H., 2009. Warm and wet conditions in the Arctic region during Eocene Thermal Maximum 2. Nat. Geosci. 2, 777–780. doi:10.1038/ngeo668.

Smith, S.Y., Manchester, S.R., Samant, B., Mohabey, D.M., Wheeler, E., Baas, P., Kapgate, D., Srivastava, R., Sheldon, N., 2015. Integrating paleobotanical, paleosol, and stratigraphic data to study critical transitions: a case study from the Late Cretaceous–Paleocene of India. Paleontol. Soc. Pap. 21, 137–166. doi:10.1017/S1089332600002990.

Sprain, C.J., Renne, P.R., Vanderkluysen, L., Pande, K., Self, S., Mittal, T., 2019. The eruptive tempo of Deccan volcanism in relation to the Cretaceous Paleogene boundary. Science 363, 866–870. doi:10.1126/science.aav1446.

Srivastava, G., Bhatia, H., Verma, P., Singh, Y.P., Agrawal, S., Utescher, T., Mehrotra, R.C., 2024. A transient shift in equatorial hydrology and vegetation during the Eocene Thermal Maximum 2. Geosci. Front. 15, 101838. doi:10.1016/j.gsf.2024.101838.

Srivastava, G., Bhatia, H., Verma, P., Singh, Y.P., Utescher, T., Mehrotra, R.C., 2023. High rainfall afforded resilience to tropical rainforests during Early Eocene Climate Optimum. Palaeogeogr. Palaeoclimatol. Palaeoecol. 628, 111762. doi:10.1016/j.palaeo.2023.111762.

Srivastava, G., Spicer, R.A., Spicer, T.E.V., Yang, J., Kumar, M., Mehrotra, R.C., Mehrotra, N.C., 2012. Megaflora and palaeoclimate of a Late Oligocene tropical delta, Makum Coalfield, Assam: evidence for the early development of the South Asia Monsoon. Palaeogeogr. Palaeoclimatol. Palaeoecol. 342-343, 130–142. doi:10.1016/j.palaeo.2012.05.002.

Svensen, H., Planke, S., Malthe-Sorenssen, A., Jamtveit, B., Myklebust, R., Eidem, T.R., Rey, S.S., 2004. Release of methane from a volcanic basin as a mechanism for initial Eocene global warming. Nature 429(6991), 542–545. doi:10.1038/nature02566.

Thakre, D., Samant, B., Mohabey, D.M., Manchester, S.R., Sangode, S., 2024. Palynology of the uppermost Cretaceous to lowermost Paleocene Deccan volcanic associated sediments of the Mandla Lobe, central India. Palynology 48(2), 2288669. doi:10.1080/01916122.2023.2288669.

Westerhold, T., Dallanave, E., Penman, D., Schoene, B., Röhl, U., Gussone, N., Kuroda, J., 2025. Earth orbital rhythms links timing of Deccan trap volcanism phases and global climate change. Sci. Adv. 11, eadr8584. doi:10.1126/sciadv.adr8584.

Wheeler, E.A., Srivastava, R., Manchester, S.R., Baas, P., 2017. Surprisingly modern latest Cretaceous–earliest Paleocene woods of India. IAWA J. 38, 456–542. doi:10.1163/22941932-20170174.

Wilf, P., Cuneo, N.R., Johnson, K.R., Hicks, J.F., Wing, S.L., Obradovich, J.D., 2003. High plant diversity in Eocene South America: evidence from Patagonia. Science 300, 122–125. doi:10.1126/science.1080475.

Wing, S.L., Bown, T.M., Obradovich, J.D., 1991. Early Eocene biotic and climatic change in interior western North America. Geology 19, 1189–1192. doi:10.1130/0091-7613.

Woodburne, M.O., Gunnell, G.F., Stucky, R.K., 2009. Climate directly influences Eocene mammal faunal dynamics in North America. Proc. Natl. Acad. Sci. USA 106, 13399–13403. doi:10.1073/pnas.0906802106.

Zachos, J.C., Dickens, G.R., Zeebe, R.E., 2008. An early Cenozoic perspective on greenhouse warming and carbon cycle dynamics. Nature 451, 279–283. doi:10.1038/nature06588.

Zachos, J., Pagani, M., Sloan, L., Thomas, E., Billups, K., 2001. Trends, rhythms and aberrations in global climate 65 Ma to present. Science 292, 686–693. doi:10.1126/science.1059412.